Viser Technology Pte. Ltd.
Research and Application of Materials Science
DOI: 10.33142/rams.v3i1.4492

Research Article Open Access

Coal Based Carbon Dots for Fe^{3+} Detection and Photoelectric Catalysis

Jianzhe JIANG[1], Zheng WANG[2], Shangwen MA [3], Gengxiong A [3], Ruiqi FENG[1], Tiezhen REN[1*]

1. School of Chemical Engineering, Hebei University of Technology, Tianjin 300130, China.
2. State Key Laboratory of High-effifiiciency Utilization of Coal and Green Chemical Engineering, Ningxia University, Yinchuan 750021, Ningxia, China
3. Bayingol vocational and technique school, Korla 84100 ,xinjiang, china

***Corresponding author:** Tiezhen REN, E-mail: rtz@hebut.edu.cn*

Abstract:
The carbon dots (CDs) could be applied in advanced field by using their sensitivity of the optical phenomenon. In this paper, the CDs in an average size of 3.75 nm was synthesized from coal by one-step solvothermal method, in which ethylenediamine was a reaction solvent and a nitrogen-containing precursor in the system. A blue-green fluorescence appeared under ultraviolet light. The strongest fluorescence emission was recorded at 480 nm under the excitation wavelength of 400 nm. The coal-based CDs could specifically recognize Fe^{3+} and the detection limit was 0.103 μM. The coal-based CDs/TiO_2 composite displayed an improved photoelectric response in 4 times comparing that of the TiO_2 under the ultraviolet light with intensity of 10 mW cm^{-2}. The photocatalytic activity over the degradation of organic molecules was accelerated as well.
Keywords: *solvothermal; carbon dots; Fe^{3+} detection; photocurrent response; photodegradation*

1 Introduction

Carbon dots (CDs) possess the unique optical properties, stable chemical properties, good bio-compatibility and excellent opto-electronic properties [1-2]. At present, carbon sources, such as graphite, carbon nanotubes, organic molecuels and biomass material etc., have been applied for CDs preparation [3-6]. On the surface of the CDs the abundant functional groups can specifically recognize metal ions. The CDs from citric acid and melamine exhibited the Fe^{3+} detection limit around 142 nM [5]. CDs from citric acid and glycine represented the Fe^{3+} detection through the phenolic hydroxyl group [6].

On the other hand, CDs are composed the conjugated π structure, which can effectively improve the photocatalytic activity and photoelectric conversion in the visible light region. CDs modified TiO_2 nanoparticles (P25) in one-step hydrothermal technique were interconnected by Ti-O-C bonds and exhibited higher efficiency than the P25 powder for the photocatalytic hydrogen production [7].

Among the carbon sources of synthetic CDs, coal has unique advantages in terms of carbon content, large reserves and low price [8-12]. The coal-based CDs were obtained through acid oxidation [8]. When mixed with TiO_2 they could effectively photodegrade organic pollutants under the sunlight and 81.2 % degradation could be achieved. The CDs with graphite microcrystal structure was obtained by the carbonization of coal and their sizes at 1.96 nm, 2.27 nm and 3.10 nm were controlled through chemically cutting coal. The sp^2 carbon domain structure and surface defects were responsible to the fluorescence emission [10]. The CDs by nitrification treatment of coal pitch and a solvent heat treatment displayed an orange fluorescence in aqueous solution [11]. While, the strong acid solution oxidation for CDs preparation caused the environment pollution seriously. It is still of great significance to explore more efficient preparation process to fulfill the large-scale preparation of CDs.

In this paper, we prepared fluorescent CDs from coal by one step solvothermal method in the absence of strong acid. The ethylenediamine was used as both the solvent and the nitrogen-containing precursor. The coal-based CDs represented a blue-green fluorescence under ultraviolet light and exhibited the strongest fluorescent emission peak at 480 nm at the optimal excitation wavelength of 400 nm, which was sensitive to

Copyright © 2021 by author(s) and Viser Technology Pte. Ltd. This is an Open Access article distributed under the terms of the Creative Commons Attribution-NonCommercial 4.0 International License (http://creativecommons.org/licenses/by-nc/4.0/), permitting all non-commercial use, distribution, and reproduction in any medium, provided the original work is properly cited.
Received on March 9, 2021; Accepted on April 16, 2021

the detection of Fe^{3+}. In addition, the CDs-TiO_2 composite displayed an efficient photosensitivity, suggesting an excellent application of photosensitive material.

2 Experimental

2.1 Preparation of coal-based CDs for Fluorescence detection

All the precursors were used without pretreatment. 0.1 g of coal to 6 mL of absolute ethanol and 4 mL of ethylenediamine were mixed with stirring for 30 mins. The mixture was then transferred to a Teflon-lined reactor and kept at 180 ℃ for 12 h. After cooling to the room temperature the obtained solution was subjected to rotary evaporation to remove excess solvent and then purified through a 0.22 micron filter. The final product was dried it at 150 ℃ for collecting the CDs powder. A solution in 0.5 mg mL^{-1} with absolute ethanol was prepared with CD powder and named as MCD64. The same protocol was used according to different ratios of ethanol and ethylenediamine solvent, and the related solution were named MCD100, MCD82, MCD55, MCD010, respectively. The control experiment was carried out without adding coal and the sample was named CD64. The pH of of the final solution was about 7. To investigate the fluorescence, we took 3 mL of CDs solution mixed with 1 mL of different ion solution. The NaCl water solution in pH range of 1-14 was adjusted by HCl (1 M) or NaOH (1 M). The metal ion solution in 5 μM (Ba^{2+}, Fe^{3+}, Ni^{2+}, Cu^{2+}, Mn^{2+}, Cr^{3+}, Co^{2+}, Zn^{2+}, K^{+}, Mg^{2+}, and Na^{+}) were tested under the same conditions. All these solution system was standing at room temperature for 5 minutes and then the fluorescence emission spectrum was measured at an excitation wavelength of 400 nm.

2.2 Characterizations

The UV-vis absorption spectrum was collected with the TU1901 equipment and $BaSO_4$ was used for calibration. An Edinburgh Instrument FSP920 was used to record the fluorescence spectrum at room temperature. The transmission electron microscopy (TEM, JEOL JEM-2100F) recorded the morphology and size at 200 kV by dispersing the sample on the copper grid covered with carbon film. The structure of the sample was measured on X-ray diffraction (XRD, Bruker D8 Advance diffractometer) with Cu radiation (λ = 0.154 nm) and the 2θ range was set from 5 to 80 °. The Fourier transform infrared (FTIR) spectra were carried out on a Bruker VERTEX 70 instrument with KBr tablet. The carbon surface chemistry of CDs was recorded by the X-ray photoelectron spectra (XPS, Physical Electronics PHI 5000 Versa Probe II spectrometer). The sample chamber was irradiated by a monochromatic Al Kα radiation (50 W, 15 kV, 1486.6 eV) after evacuated to $5.2*10^{-9}$ mbar. The C1s photoelectron line at 284.8 eV was used to calibrate the spectrometer energy scale. To determine the binding energy of different element core energy levels accurately, the deconvolution was performed with Gauss-Lorentz model.

2.3 Preparation and performance of MCD64/TiO_2 composite photoelectric materials

2 ml of MCD64 (0.5 mg mL^{-1}) was mixed with 8 ml of distilled water, followed by addition of 100 mg of TiO_2 powder at room temperature for 2 hours to obtain a homogeneous suspension. The suspension was then transferred to a 30 mL stainless steel Teflon reactor and held at 140 ℃ for 4 hours. After cooling to room temperature, the obtained product was centrifuged at 3000 rpm for 10 minutes to collect a solid sample, which was washed twice with absolute ethanol, and finally dried at 50 ℃ to obtain MCD64/TiO_2 complex. Then its uniform suspension was prepared with ethanol and evenly coated on the ITO conductive glass within an effective area of 2 cm^2. Subsequently, the membrane was dried in a constant temperature oven at 150 ℃ for 30 minutes to increase the adhesion of the surface. This ITO glass covered with MCD64/TiO_2 was used as the working electrode for the investigation of the photocurrent response. Photoelectric response was tested with IM6&ZENNIUM (Zahner) electrochemical workstation and UV light emitting diode (UVR01, 390 nm) with intensity of 10 mW cm^{-2}. The working electrode of ITO glass was assembled in a three-electrode system with Pt as a counter electrode and Ag/AgCl as a reference electrode. 0.2 M of Na_2SO_4 solution was used as the electrolyte. The Electrochemical impedance spectroscopy (EIS) was evaluated with the frequency range from 10 mHz to 30 kHz with a perturbation amplitude of 5 mV.

3 Results and discussion

3.1 Fluorescence properties of prepared coal-based CDs under different systems and detection of metal ions

The CDs were formed with the ratio change of ethanol and ethylenediamine, in which the coal powder was the basic materials. The sample represents blue color under daylight and light yellow color under UV-light (Figure 1a). MCD64 has the strongest fluorescence intensity at 480 nm among those samples as represented in Figure 1b. The UV absorption curves of those samples present two absorption peaks at 255 nm and 347 nm (Figure 2c). The UV spectra (Figure 2d) of CD64 has two weak absorption peaks at 255 nm and 347 nm. The corresponding fluorescence emission spectrum (Figure 2e) of CD64 represents a weak intensity peak at 480 nm as well, suggesting that the coal powder and ethylenediamine contributes to the formation of CDs.

The CDs were formed with the ratio change of ethanol and ethylenediamine, in which the coal powder was the basic materials. The sample represents blue color under daylight and light yellow color under UV-light

(Figure 1a). MCD64 has the strongest fluorescence intensity at 480 nm among those samples as represented in Figure 1b. The UV absorption curves of those samples present two absorption peaks at 255 nm and 347 nm (Figure 2c). The UV spectra (Figure 2d) of CD64 has two weak absorption peaks at 255 nm and 347 nm. The corresponding fluorescence emission spectrum (Figure 2e) of CD64 represents a weak intensity peak at 480 nm as well, suggesting that the coal powder and ethylenediamine contributes to the formation of CDs.

The CDs were formed with the ratio change of ethanol and ethylenediamine, in which the coal powder was the basic materials. The sample represents blue color under daylight and light yellow color under UV-light (Figure 1a). MCD64 has the strongest fluorescence intensity at 480 nm among those samples as represented in Figure 1b. The UV absorption curves of those samples present two absorption peaks at 255 nm and 347 nm (Figure 2c). The UV spectra (Figure 2d) of CD64 has two weak absorption peaks at 255 nm and 347 nm. The corresponding fluorescence emission spectrum (Figure 2e) of CD64 represents a weak intensity peak at 480 nm as well, suggesting that the coal powder and ethylenediamine contributes to the formation of CDs.

The absorption peak of UV absorption at 255 nm (Figure 2a) is derived from the π-π* transition of the sp^2 hybrid carbon [13]. The second peak at 347 nm attributes to the n-π* transition of the C=O bond on the surface of MCD64 [14]. The optimal excitation wavelength of MCD64 is 400 nm, which is in good symmetry with the fluorescence emission spectrum (480 nm) at the excitation wavelength of 400 nm. Figure 2b shows that the fluorescence center of MCD64 shifts from 475 nm to 505 nm with the excitation wavelength increasing from 380 nm to 460 nm. The highest response of fluorescence is at 480 nm when excitation wavelength set at 400 nm. Such excitation-dependent fluorescence is related to defects on the surface of the CDs and optimizing the excitation wavelength is necessary [15].

Figure 2c shows that the intensity of MCD64 becomes weak with a blue shift under the acid/alkali environment. The good stability of CDs in NaCl solution relates to the application under complex conditions. The fluorescence emission spectrum measured at λ_{ex} = 400 nm represents the peak position in consistency, as shown in Figure 2c (inset). The peak intensity of all the curves at different concentration from 0 M to 2.5 M is almost the same. However, at different pH value the fluorescence feature of MCD64 varies obviously (Figure 2d). Around 30 - 35 % decrease is recorded when pH at 1 or 14, suggesting that the surface functional group of CDs might be reacted with proton or hydroxide and weaken the fluoresence [4]. The suitable condition for MCD64 locates in the pH range of 6-9 with a high response of the fluorescence.

The application of the CDs could be applied to discriminate the metal ions in the solution by the variation of fluorescence. The fluorescence intensity of CDs was measured at 400 nm excitation wavelength by adding 5 μM of Ba^{2+}, Fe^{3+}, Ni^{2+}, Cu^{2+}, Mn^{2+}, Cr^{3+}, Co^{2+}, Zn^{2+}, Mg^{2+}, Na^{+}, K^{+} solutions to MCD64 solution. Figure 2e clearly shows that only Fe^{3+} has a significant fluorescence quenching effect on the fluorescence intensity of MCD64. The rest metal ions have only a slight effect on the fluorescence intensity. This indicates that MCD64 can specifically recognize Fe^{3+}.

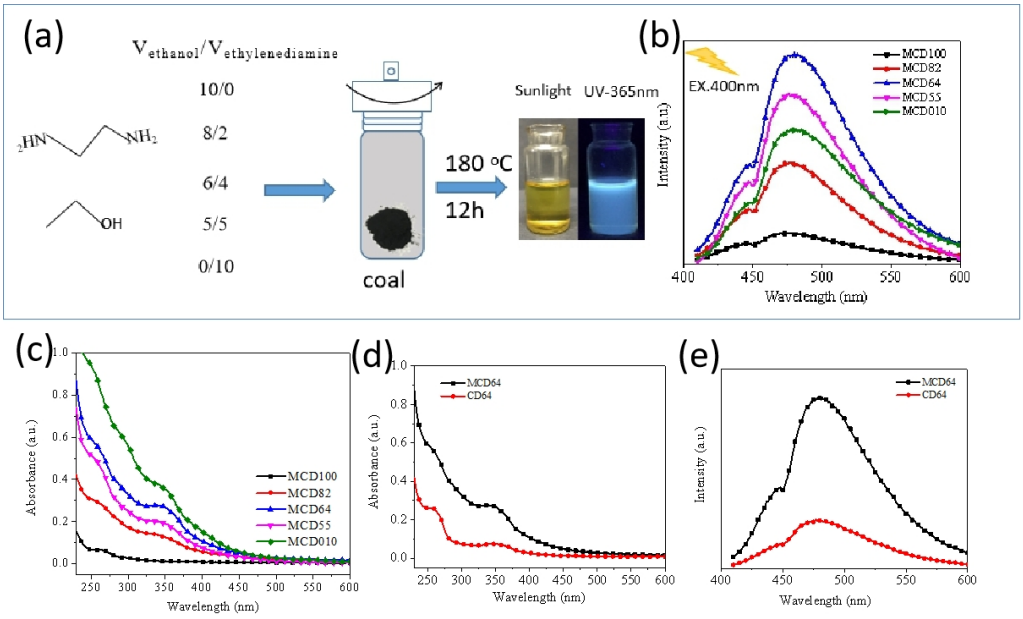

Figure 1 The scheme of synthesis route for CDs with the fluorescence characters (a), the fluorescence emission spectrum at 400 nm excitation wavelength (b), UV absorption curve of coal-based CDs under different systems and (inset) a picture of the sample under 365 nm UV lamp (c), The UV absorption spectra (d) and the fluorescence emission spectrum at an excitation wavelength of 400 nm (e) of the MCD64 and CD64

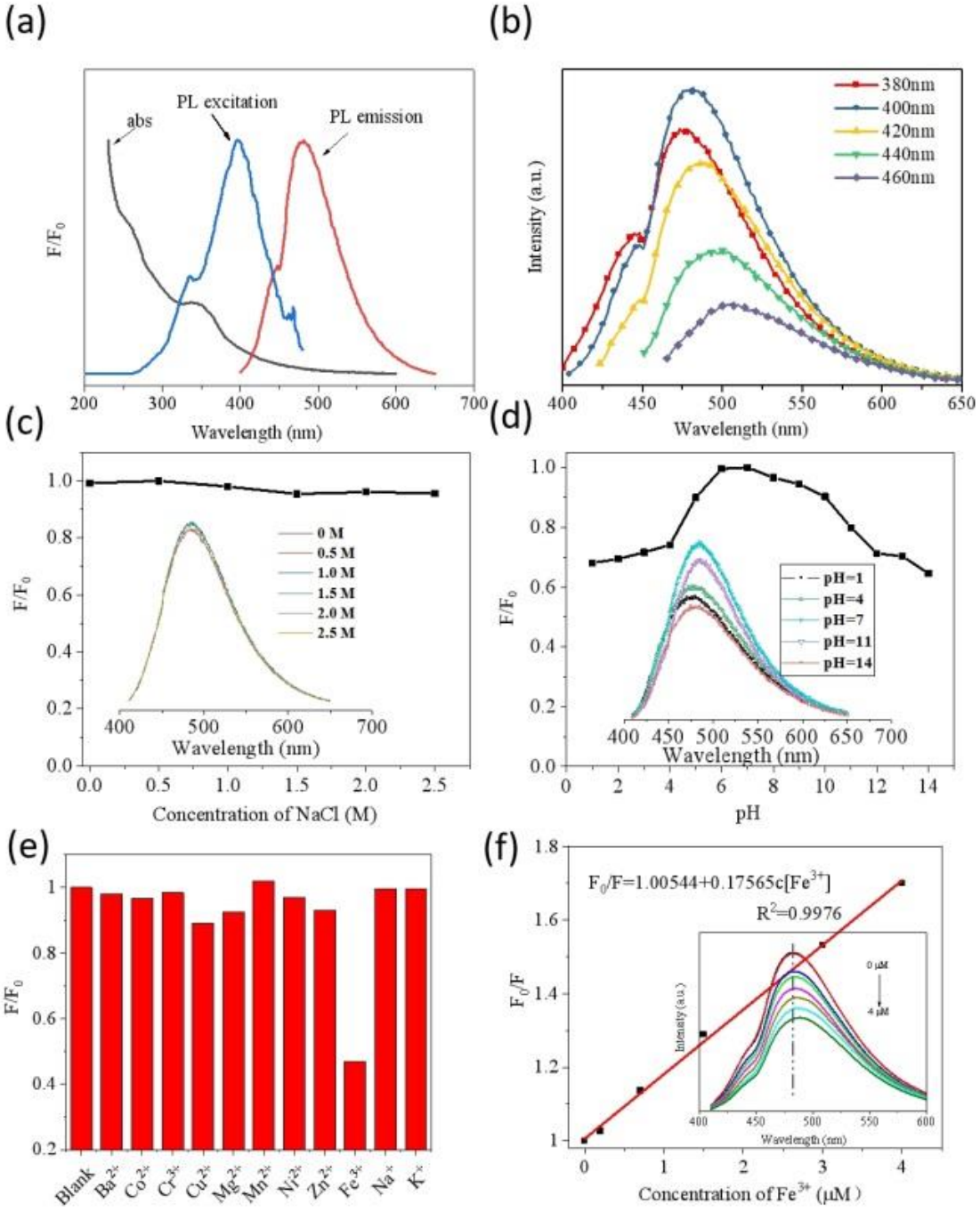

Figure 2 (a) UV-vis spectrum, excitation spectrum and fluorescence emission spectrum of MCD64; (b) Fluorescence emission spectrum of MCD64 at different excitation wavelengths. (c) Effect of NaCl concentration and (inset) The fluorescence curves of CDs in NaCl solution. (d) pH on fluorescence property of CDs and (inset) The fluorescence curves of CDs at different pH solution. (e) Relative PL intensity diagram of MCD64 after adding different kinds of metal ions. (f) Fitting curve for relative PL intensity and (inset) Emission spectrum of MCD64 with Fe^{3+} in the range of 0-4 μM

The specific selection to Fe_{3+} is further evaluated with investigation of the sensitivity. The fluorescence intensity change of the MCD64 and the concentration of Fe3+ were linearly fitted based on the Stern-Walmer equation, and the fitting equation was F0/F=1.00544+0.17565c[Fe_{3+}] (R2=0.9976), as shown in Figure 2f. As shown in Figure 2f (inset), the fluorescence intensity of the MCD64 gradually decreases with the Fe_{3+} concentration increases from 0 to 4 μM. The detection limit was calculated according to 3 N/k (N is the standard deviation of the fluorescence intensity of the blank sample, k is the slope of the linear fitting equation), and the detection limit is 0.103 μM. The detection limit is better than the detection limit of Fe_{3+} (0.21 μM) of

GCDs, which was obtained by hydrothermal treatment of citric acid and glycine [6]. We believe that the CDs with specific surface states decide the detection limits and detection ranges for Fe_{3+}.

3.2 Structural characterization of coal-based CDs

The XRF spectra of coal and MCD-64 revealed the difference between the coal and CDs. Figure 3a shows that the coal has weak peaks at 2.31 keV, 3.69 keV, 4.51 keV and 5.90 keV, corresponding to S, Ca, Ti and Mn elements, respectively. The two peaks at 6.41 keV and 7.11 keV are generated by the α and β emission lines of the Fe element. It is worth noting that the Ar element at 2.96 keV is derived from air. After solvent heat treatment and post-purification treatment the MCD64 represents only the Ar element in the spectra, indicating that no impurities exist in the sample.

The TEM image shows that MCD64 are approximately in spherical shape and dispersed well (Figure 3c). The sizes are all less than 10 nm, mainly concentrated in 2-5 nm, and the average particle size is 3.75 nm (Figure 3c inset). The Figure 3d shows the FT-IR spectra of MCD64 and coal. A significant broad peak at 3435 cm^{-1} of MCD64 is the characteristic peak -OH and -NH bonds [17], which is much stronger than that of coal. This indicates that more hydrophilic groups are formed on the surface of MCD64 during the hydrothermal process, and ensure a good water solubility and stability of MCD64 [18]. The absorption peak of the C-H bond located at 3020 cm^{-1} is observed in MCD64, other than that of the coal, confirming the small sp^2 hybrid carbon stripped from the coal [19]. The characteristic peaks at 1616 cm^{-1} and 1409 cm^{-1} can be attributed to the absorption of the C=O bond and the C=C skeleton [5,20]. 1126 cm^{-1} is ascribed to the absorption of C-N bond [13], indicating that the N element from ethylenediamine is successfully introduced to the surface of MCD64. The characteristic peak at 1010 cm^{-1} is attributed to the absorption of the C-OH bond [17], indicating the presence of phenolic hydroxyl groups on the surface of the CDs. Thus MCD64 were successfully prepared based on the existence of the coal powder. Similar to the CDs from citric acid and glycine [6], the surface phenolic hydroxyl groups could react with Fe^{3+} to form a polymer, then the excited state electrons of the CDs transfer to the d-state orbit of Fe^{3+} and the electron-hole pairs recombined, leading to a fluorescence quenching of the CDs.

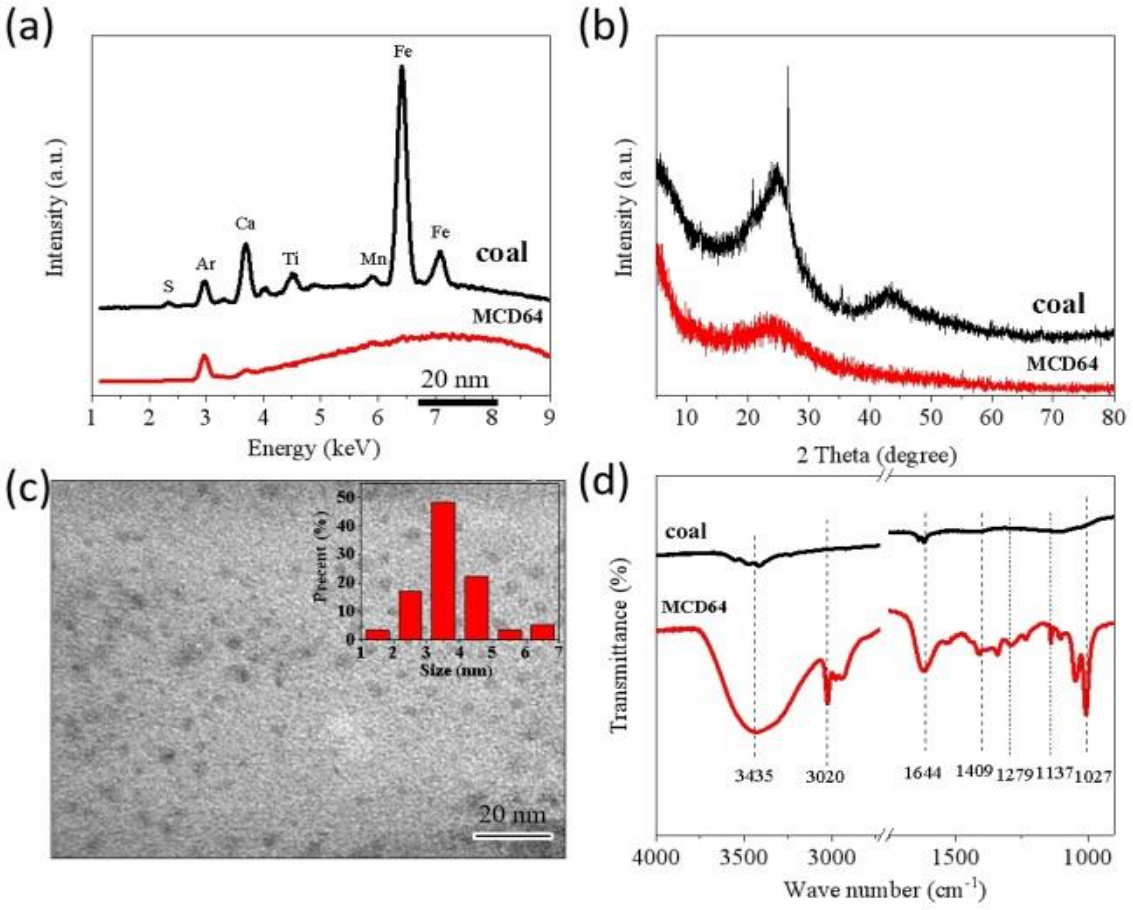

Figure 3 XRF patterns (a) and XRD patterns (b) of coal and MCD64, (c) TEM spectrum and size distribution map of MCD64 (inset) and (d) FTIR spectrum of coal and MCD64 samples

3.3 photoelectric performance analysis of composite photoelectric materials

The CDs could be used as the heteroatoms to improve the photoelectric response of metal oxides [21-24]. Figure 4a shows the energy band curve of the MCD64 modified TiO_2, which is calculated according to the UV-absorption spectrum. The band width of MCD64/TiO_2 is reduced to 2.84 eV from 3.2 eV of TiO_2, suggesting that the doped CDs can effectively accelerate the transition of electrons and generate electron-hole pairs to improve the photoelectric response [25,26].

The fluorescence emission spectroscopy can also be used to characterize the photo-generated charge of photovoltaic materials. The lower fluorescence intensity fits to the less photoelectron recombination efficiency [27]. As shown in Figure 4b, the fluorescence center of the MCD64 sample is at 480 nm at the excitation wavelength of 400 nm, and the emission peak intensity of MCD64/TiO_2 at 480 nm is significantly decreased. The photoelectron recombination efficiency of the composite is reduced, and the presence of coal-based CDs acts to suppress the photoelectron-hole pair recombination of TiO_2, thereby improving the photoelectric characteristics [24]. Therefore, these results indicate that the prepared coal-based CDs can act as a sensitizer in the composite photovoltaic material, enhance the absorption of visible light and promote the charge transfer efficiency, thereby increasing the possibility of application in photovoltaic materials.

Figure 4c represents that the photoelectric current of TiO_2 is 0.14 μA cm^{-2} under UV light with a light intensity of 10 mW cm^{-2}. After doping MCD64, the photoelectric current is significantly improved to 0.55 μA cm^{-2}, which is about 4 times than that of TiO_2. We believe that CDs is irradiated by the ultraviolet lamp, the electron absorption energy transitions to the excited state, and can be quickly transferred to the conduction band of the TiO_2, thereby enhancing the photoelectric response of the composite photoelectric material. The degradation in dark was monitored and the slight increased degradation can be observed (Figure 4d). After the subtraction of the degradation in dark, the degradation rate of MCD64/TiO_2 sample to methylene blue under the UV irradiation for 3.5 hours. A decrease at 75 % was observed with MCD64/TiO_2, which shows a 20 % of augmentation control to the TiO_2 sample.

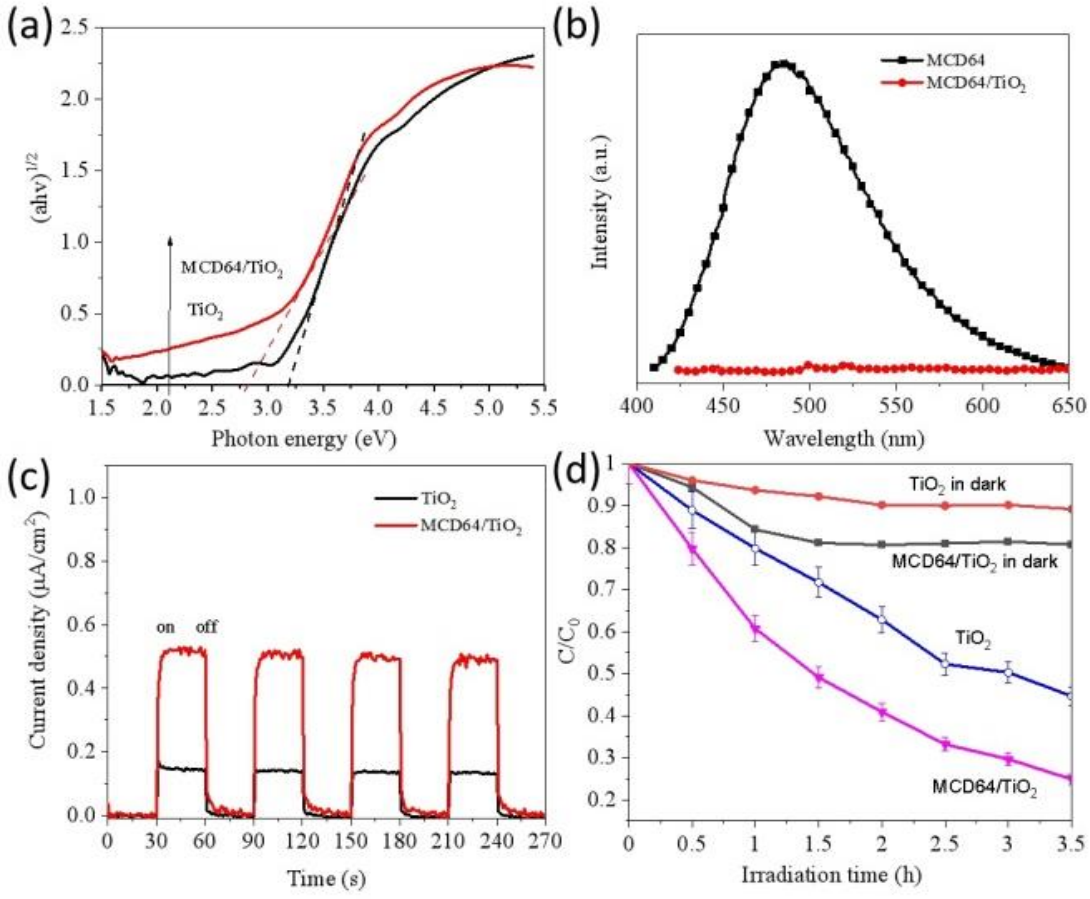

Figure 4 (a) Band gap curve of TiO_2 and MCD64/TiO_2, (b) fluorescence emission spectrum, (c) Photoelectric response of TiO_2 and MCD64/TiO_2, and (d) Methylene blue degradation in dark and UV light

The fluorescence emission spectroscopy can also be used to characterize the photo-generated charge of photovoltaic materials. The lower fluorescence intensity fits to the less photoelectron recombination efficiency [27].

As shown in Figure 4b, the fluorescence center of the MCD64 sample is at 480 nm at the excitation wavelength of 400 nm, and the emission peak intensity of MCD64/TiO_2 at 480 nm is significantly decreased. The photoelectron recombination efficiency of the composite is reduced, and the presence of coal-based CDs acts to suppress the photoelectron-hole pair recombination of TiO_2, thereby improving the photoelectric characteristics [24]. Therefore, these results indicate that the prepared coal-based CDs can act as a sensitizer in the composite photovoltaic material, enhance the absorption of visible light and promote the charge transfer efficiency, thereby increasing the possibility of application in photovoltaic materials.

Figure 4c represents that the photoelectric current of TiO_2 is 0.14 μA cm^{-2} under UV light with a light intensity of 10 mW cm^{-2}. After doping MCD64, the photoelectric current is significantly improved to 0.55 μA cm^{-2}, which is about 4 times than that of TiO_2. We believe that CDs is irradiated by the ultraviolet lamp, the electron absorption energy transitions to the excited state, and can be quickly transferred to the conduction band of the TiO_2, thereby enhancing the photoelectric response of the composite photoelectric material. The degradation in dark was monitored and the slight increased degradation can be observed (Figure 4d). After the subtraction of the degradation in dark, the degradation rate of MCD64/TiO_2 sample to methylene blue under the UV irradiation for 3.5 hours. A decrease at 75 % was observed with MCD64/TiO_2, which shows a 20 % of augmentation control to the TiO_2 sample.

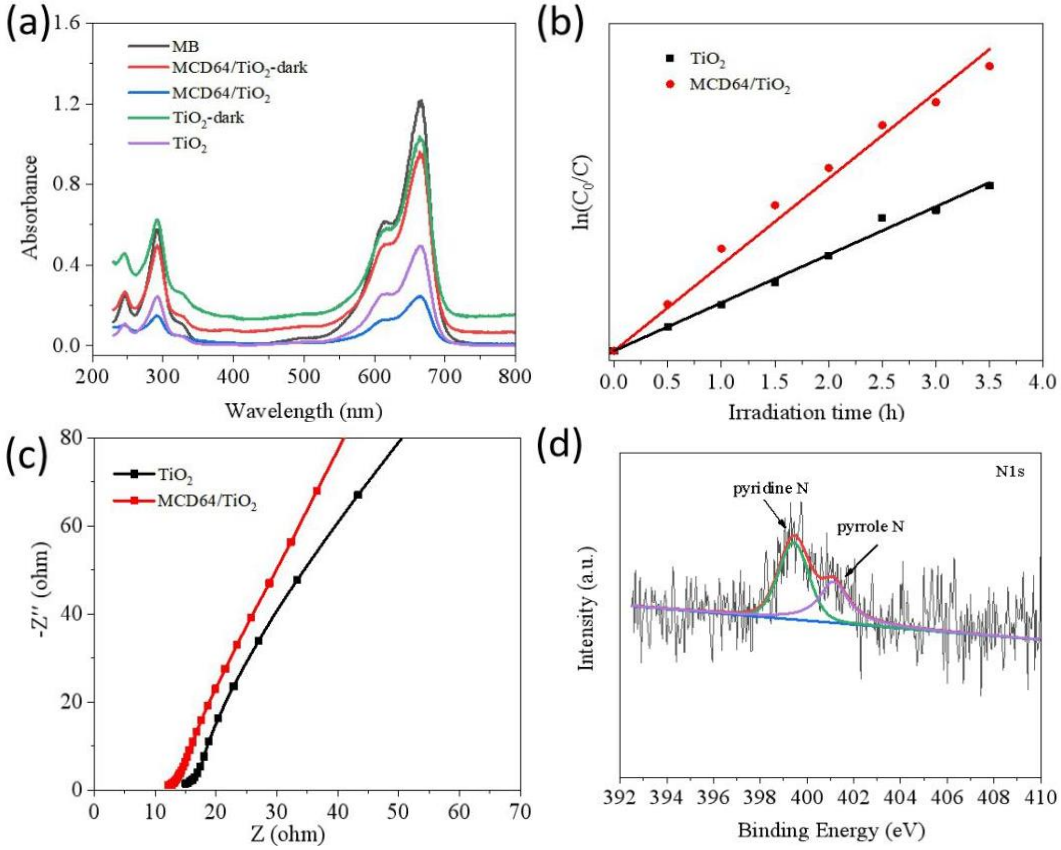

Figure 5 (a) Methylene blue adsorption curve under different condition, (b) the kinetic study equation of of MCD64/TiO_2 and TiO_2 samples, (c) Nyquist plot, (d) XPS survey spectra N1s of MCD64/TiO_2

The photocatalytic degradation characteristics of MCD64/TiO_2 and TiO_2 materials to methylene blue under ultraviolet light were studied. The control experiment was performed with the observation of the absorbance of UV-vis spectra (Figure 5a).The kinetic study of the adsorption data, as shown in Figure 5b, shows a good linear relationship between ln (C_0/C) and t, which means that the photodegradation process of methylene blue on the photocatalyst follows the rules of first-order reaction kinetics. The apparent reaction rate constant of MCD64/TiO_2 and TiO_2 is 0.42 and 0.23 h^{-1}, respectively, reflecting the promoted photocatalytic degradation process with the coal-made CDs.

The conjugated π structure in the CDs can effectively improve the photocatalytic activity and photoelectric conversion characteristics of the semiconductor material, and can be a new type of photovoltaic material after being chemically combined with TiO_2 [24]. The photocatalytic properties of TiO_2 are derived from electron-hole pairs generated by illumination, the holes generated in the valence band (VB) have strong oxidizing properties and are easy to capture electrons in the solvent, and the photoelectrons on the conduction band (CB) are reducible and undergo oxidation-reduction reaction with organic molecules in the solvent to achieve the purpose of catalysis [22, 23].

Therefore, the combination of TiO_2 with a suitable material suppresses the recombination of the VB electrons and the holes of the CB. An intense redox reaction occurs on the surface of the composite material, enhancing the photocatalytic activity.

The influence of CDs was further confirmed by electrochemical impedance spectroscopy (EIS). The Nyquist plots of MCD64/TiO_2 and TiO_2 are shown in Figure 5c. Since only a single half ring is observed, the equivalent resistance and charge transfer resistance (R_s+R_{ct}) of the electrode material are reflected in the intercept of the high frequency region curve and the real axis [26] Compared with TiO_2 powder (15 Ω), the composite sample (12 Ω) has smaller equivalent resistance and charge transfer resistance, indicating that the composite optoelectronic material has more efficient charge transfer efficiency. To confirm the effect of ethylenediamine for the formation of MCD64, the XPS survey spectra was investigated. Nitrogen in the sample is 0.97 at%. The high-resolution N1s spectrum possesses two peaks at 399.4 eV and 401.1 eV, ascribing to pyrrole N and pyridine N-oxides [28], respectively. Thus the N element from ethylenediamine is successfully introduced into the CDs (Figure 5d).

The coal is a macromolecular substance formed by the sp^2 carbon domains through fat chains. During the solvothermal reaction, the high temperature and high pressure environment cause the fatty chain break, and the small debris of carbon nanoparticle from the coal is peeled off with sp^2 structure [13]. At the same time, the ethylenediamine and ethanol could be splited in solvothermal system, thus the functional groups with N atoms improve the fluorescence performance of the CDs [29]. Compared with the strong acid oxidation etching or hydrogen peroxide oxidation preparation process, the solvothermal method easily lead to the formation of CDs with oxygen-containing functional groups. The conjugated structures inhibit non-radioactive recombination of electron-hole pairs [30], resulting in a superior fluorescence performance.

4 Conclusions

We prepared a fluorescent carbon dots with a size of 3.75 nm from coal by one-step solvothermal method. The ethylenediamine was used as both a reaction solvent and a nitrogen-containing precursor in the system. The coal-based CDs showed blue-green fluorescence under ultraviolet light. The coal-based CDs displayed the strongest fluorescence emission at 480 nm under the optimal excitation wavelength of 400 nm, which was sensitive to the Fe^{3+} ions under different circumstance. The coal-based CDs-TiO_2 composite possessed the photoelectric response higher than the TiO_2 four times under the ultraviolet light with intensity of 10 mW cm^{-2}. It was effective to the photodegradation of methylene blue with a increase of 20 % comparing to the TiO_2. The coal-based CDs acted as a sensitizer and could effectively enhance the conductive charge transfer rate, which enhanced the photoelectric response of the composite photovoltaic material.

Acknowledgement: This work was supported by the Foundation of State Key Laboratory of High efficiency Utilization of Coal and Green Chemical Engineering, Ning Xia University (2020-KF-22), Special project of Science and Technology Department, Xinjiang Uygur Autonomous Region (2020D03025) and the Natural Science Foundation of Xinjiang Uygur Autonomous Region (2021D01A03).

References

[1] Hu S, Wei Z, Chang Q, et al. Facile and green method towards coal-based fluorescent carbon dots with photocatalytic activity. Applied Surface Science 2016, 378: 402-407.

[2] Namdari P, Negahdari B, Eatemadi A. Synthesis, properties and biomedical applications of carbon-based quantum dots: An updated review. Biomedicine & pharmacotherapy, 2017, 87: 209-222.

[3] Molaei M J, A review on nanostructured carbon quantum dots and their applications in biotechnology, sensors, and chemiluminescence. Talanta 2019, 196: 456-478.

[4] Sun C, Zhang Y, Wang P, et al. Synthesis of Nitrogen and Sulfur Co-doped Carbon Dots from Garlic for Selective Detection of Fe^{3+}. Nanoscale research letters 2016, 11(1): 110.

[5] Liu S, Liu R, Xing X, et al. Highly photoluminescent nitrogen-rich carbon dots from melamine and citric acid for the selective detection of iron(III) ion. Rsc Advances 2016, 6(38): 31884.

[6] Feng R Q, Yuan Z Y, Ren T Z. A facile hydrothermal method for preparation of fluorescent carbon dots on application of Fe^{3+} and fingerprint detection. Methods and applications in fluorescence 2019, 7(3): 35001.

[7] Yu H, Zhao Y, Zhou C, et al. Carbon quantum dots/TiO_2 composites for efficient photocatalytic hydrogen evolution. Journal of Materials Chemistry A 2014, 2(10): 3344-3351.

[8] Zhang B, Halidan M, Zhang D, et al. Preparation of coal-based C-Dots/TiO_2 and its visible-light photocatalytic characteristics for degradation of pulping black liquor. Journal of Photochemistry and Photobiology a-Chemistry 2017, 345: 54-62.

[9] Hoang, V. C, Hassan, M, Gomes, V. G., Coal derived carbon nanomaterials – Recent advances in synthesis and applications. Applied Materials Today 2018, 12, 342-358.

[10] Hu C, Yu C, Li M, et al. Chemically tailoring coal to fluorescent carbon dots with tuned size and their capacity for Cu (II) detection. Small 2014, 10(23): 4926-4933.

[11] Geng B, Yang D, Zheng F, et al. Facile conversion of coal tar to orange fluorescent carbon quantum dots and their composite encapsulated by liposomes for bioimaging. New Journal of Chemistry 2017, 41 (23): 14444-14451.

[12] Zhang B, Halidan M, Zhang Y F, et al. Preparation of Coal-based C-dots and Their Application in Trace Cu(II) Detection. Chinese Journal of Analytical Chemistry 2017, 45 (10): 1489-1496.

[13] Li M, Hu C, Yu C, et al. Organic amine-grafted carbon quantum dots with tailored surface and enhanced photoluminescence properties. Carbon 2015, 91: 291-297.

[14] Li M, Yu C, Hu C, et al. Solvothermal conversion of coal into nitrogen-doped carbon dots with singlet oxygen generation and high quantum yield. Chemical Engineering Journal 2017, 320: 570-575.

[15] Liu Q, Zhang J, He H, et al. Green Preparation of High Yield Fluorescent Graphene Quantum Dots from Coal-Tar-Pitch by Mild Oxidation. Nanomaterials 2018, 8 (10): 844.

[16] Thiyagarajan S K, Raghupathy S, Palanivel D, et al. Fluorescent carbon nano dots from lignite: unveiling the impeccable evidence for quantum confinement. Physical Chemistry Chemical Physics 2016, 18 (17): 12065-12073.

[17] Gu D, Shang S, Yu Q, et al. Green synthesis of nitrogen-doped carbon dots from lotus root for Hg(II) ions detection and cell imaging. Applied Surface Science 2016, 390: 38-42.

[18] Singamaneni S R, Van T J, Ye R, et al. Intrinsic and extrinsic defects in a family of coal-derived graphene quantum dots. Applied Physics Letters 2015, 107: 212402.

[19] Li H, Guo X, Liu J, et al. A synthesis of fluorescent starch based on carbon nanoparticles for fingerprints detection. Optical Materials 2016, 60: 404-410.

[20] Dutta Chowdhury A, Doong R A. Highly Sensitive and Selective Detection of Nanomolar Ferric Ions Using Dopamine Functionalized Graphene Quantum Dots. ACS applied materials & interfaces 2016, 8 (32): 21002-10.

[21] Zhuo S, Shao M, Lee S T. Upconversion and Downconversion Fluorescent Graphene Quantum Dots: Ultrasonic Preparation and Photocatalysis. Acs Nano 2012, 6(2): 1059-1064.

[22] Li Y, Xia Y, Liu K, et al. Constructing Fe-MOF-Derived Z-Scheme Photocatalysts with Enhanced Charge Transport: Nanointerface and Carbon Sheath Synergistic Effect [J]. ACS Applied Materials & Interfaces, 2020, 12: 25494−25502.

[23] Huang Y, Guo Z, Liu H, et al. Heterojunction Architecture of N‐Doped WO_3 Nanobundles with Ce_2S_3 Nanodots Hybridized on a Carbon Textile Enables a Highly Efficient Flexible Photocatalyst[J]. Advanced Functional Materials, 2019, 29(45), 1903490.

[24]. Zhou J, Chen J, Zheng J, et al. Role of carbon quantum dots in titania based photoelectrodes: Upconversion or others? Journal of colloid and interface science 2018, 529: 396-403.

[25] Zhang Y, Zeng W, Ye H, et al. Enhanced carbon monoxide sensing properties of TiO_2 with exposed (001) facet: A combined first-principle and experimental study. Applied Surface Science 2018, 442: 507-516.

[26] Babar P T, Lokhande A C, Pawar B S, et al. Electrocatalytic performance evaluation of cobalt hydroxide and cobalt oxide thin films for oxygen evolution reaction. Applied Surface Science 2018, 427: 253-259.

[27]Cheng C, Lu D, Shen B, et al. Mesoporous silica-based carbon dot/TiO_2 photocatalyst for efficient organic pollutant degradation. Microporous and Mesoporous Materials 2016, 226: 79-87.

[28] Xu S, Qiu S, Yuan Z, et al. Nitrogen-containing activated carbon of improved electrochemical performance derived from cotton stalks using indirect chemical activation[J]. Journal of Colloid And Interface Science,2019, 540: 285-294.

[29] Zhai X, Zhang P Liu, C Bai, et al. Highly luminescent carbon nanodots by microwave-assisted pyrolysis. Chemical communications 2012, 48 (64): 7955-7.

[30] Ming H, Ma Z, Liu Y, et al. Large scale electrochemical synthesis of high quality carbon nanodots and their photocatalytic property. Dalton Transactions 2012, 41(31): 9526-9531.